SSRG International Journal of Electrical and Electronics Engineering
ISSN: 2348 – 8379 / https://doi.org/10.14445/23488379/IJEEE-V9I8P103

Volume 9 Issue 8, 17-27, August 2022

Original Article

Frequency Variations of Low Inertia Grid by MPPT Controller & EHHO Algorithm: A Synthetic Inertia Approach

N. Nandakumar[1], V.A. Tibbie Pon Symon[2]

[1,2]*Department of Electrical and Electronics Engineering, Noorul Islam Centre for Higher Education, Kumaracoil,*

[1] n.nandakumar24@gmail.com

Received: 16 June 2022 Revised: 12 August 2022 Accepted: 17 August 2022 Published: 31 August 2022

Abstract - *The distributed and unpredictable character of renewable energy sources is creating significant provocation for the working of the power system. Particularly when the entry of inverter-based frameworks is considerable, the integrity of the framework may be at risk. The answer to supporting the future expansion of dispersed frameworks is seen as a characteristic of capacity and the lawful strategy of regulators. To maintain the framework's unshakable quality at the highest possible level, control approaches should be designed to provide the framework with the necessary assistance and be suited for keeping the variation of recurrence inside cutoff points. The main issues include the frequency stability of present systems, minimizing delay by adding power after failure scenarios, and a lack of understanding of the distinction between inertia and rapid frequency response. This research employed the Maximum Power Point Tracking (MPPT) and advanced Harris Hawk optimization (EHHO) methods for power and frequency control in low inertia systems to increase frequency stability. Effective results are obtained from the experimental comparison of the proposed model with the existing model, like perturb and observe (P&O) algorithm.*

Keywords - *Grid System, Harris Hawk's Optimization, Renewable Energy Source, Synthetic Inertia, Maximum Power Point Tracking.*

1. Introduction

Over the past ten years, renewable energy sources (RES) have gained popularity and now makeup 22% of the world's energy consumption and much of the world's energy output. [25] In today's power networks, coal, oil, and natural gas-based power generation are gradually replaced by wind turbines and solar cells. Under the current grid standards, there are technical restrictions on distributed generation (DG) stations, especially solar (PV) plants. Compared to conventional electricity production based on synchronous machines (SM), grid-connected RES interconnections through static inverters have a restricted inertial sensitivity for grid frequency and voltage consistency because there are no spinning elements. The inertia of the grid prevents frequency fluctuations when unexpected loads or generation changes occur. System inertia, a universal property, controls how much kinetic energy the grid can store and inject. Greater frequency changes after a disruption typically follow lower inertia. Numerous methods have been described for creating virtual (or synthetic) inertia to compensate for the loss of rotational inertia [4-6]. Several control techniques have been developed to make power converters operate as closely as feasible to synchronous machines. In this study, an efficient frequency controller based on EHHO and ROCOF monitoring is utilized to enhance the frequency impulse of a negligible inertia system.

Using a conventional inverter to link RES reduces frequency stability since there are no spinning masses [1]. A fast-responding inverter is used to connect RES to the grid due to its intermittent nature, and it is delivered to the grid as a fast-dynamic system [2]. This rapid communication results in phase angle, voltage amplitude instability and frequency [3]. It produces stronger substantial-frequency motions and brief power exchanges during a power outage. To overcome the difficulties experienced by grid-linked RES, virtual inertia (VI), a sort of artificial inertia control technology, was developed and thoroughly investigated in traditional inverters. VI theoretically simulates the inertia response of a common synchronous machine using PWM. Figure 1 depicts a generic VI-based grid-connected structure.

Virtual inertia control systems [7] have recently attracted much interest. The dynamics of the VSG approach and droop control strategies [8] for simulating inertia in systems. The stability of wind turbine systems is improved

by [10] using a droop control technique to use synthetic inertia as an additional inertia response. The control system [11] accounts for the inertia of the European power grid. According to [11], DC microgrids should be integrated into the utility/power grid as virtually synchronous machines. A model predictive control technique based on VI control is used to increase microgrid stability.

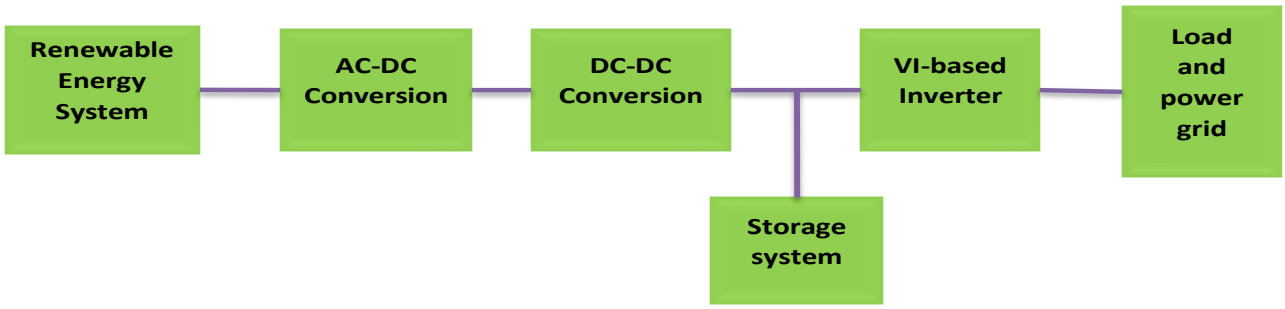

Fig. 1 Generic structure of VI-based grid-connected system

Virtual inertia management has proposed a microgrid method to guarantee frequency stability in practically all grid-connected renewable energy sources. The extensive tuning methods to identify the appropriate virtual inertia control parameters for power systems. There has never been any investigation into how transmission systems affect virtual inertia control. Most research focuses on reducing virtual inertia in small-scale or microgrid, single-area power systems. VI control for distribution and high voltage alternating current components of connected power networks has never been looked at for large-scale power systems. As renewable energy sources have expanded, interconnected power system applications have become more common, focusing on multi-area power systems to share electricity while boosting stability and reliability. Developed HVAC/HVDC tie-lines in parallel and SMES technology for several linked power networks. The materials provided state that no research has been conducted on inertia control strategies to examine the effects of inertia under high-RES penetration.

System inertia (H), which results from a mismatch between load demand and generation, is the most fundamental source of electrical system resilience in frequency control. The source of inertia is synchronous generators that are directly linked to the grid [23]. They are essential for controlling the rate of change of frequency (ROCOF) and permitting a normal reaction to changes in the system's frequency. The three most fundamental methods for controlling frequency are primary control, inertia control, and secondary control. When the frequency changes, the controllers are disabled, and the demand is satisfied by the kinetic energy of the synchronous generating units.[27] Following secondary control, the controller restores the system frequency to its equilibrium stage, depending on the circumstances.

Kinetic energy calculates the inertia response in standard system-based synchronous generators.

The following list of study objectives is included in the research technique that is being presented:

- In low-inertia power systems, the frequency stability could be increased, and the effects of noise and filtering on controller performance are investigated.
- The two best frequency control methods utilized in imbalanced power occurrences are inertial response and fast power reserve.
- Supercapacitors are being used as an energy storage option to improve grid systems, and the proposed technology provides full power availability due to enhanced frequency stability using synthetic inertia.

The source of the remaining paper is listed here: The remaining article is organized as follows because the first section provided an overview of RES and VI. The literature review is found in Section II, the technique for the proposed system is given in Section III, the analysis is provided in Section IV, and the conclusion is given in Section V.

2. Literature Review

Researchers have discussed various frequency controllers in PV systems in recent years. A brief breakdown of some of the most recent studies is presented in this section.

Kah Yung Yan et al. [28] contributed to a breakthrough in synchronverter design with ML-based VI syncretization. The reaction and critic networks were combined to create the ML-based VI shown below to discriminate between reactive and active power control. The outcomes indicated that a synchronverter powered by machine learning would be workable and efficient. The suggested management strategy decreased maximum frequency fluctuation from the nominal value by 0.1Hz, the settling time required to achieve quasi-steady-state frequency by 50%, and steady-state inaccuracy by 50%. It is challenging to connect a PV system to the electrical grid while maintaining high-frequency stability.

Sotirios et al. [26] presented the multi-stage grid-tied PV system with the frequency response and could be used in power system research. The system could operate on a designed active power reserve and drooping and inertia feedback control system, enabling under-frequency response. Simulations of the time domain were used to assess the advantages of droop type and inertia frequency controllers, along with a discussion of parameter choice. When the PV generator supplied frequency responsiveness, time-domain simulations were used to evaluate the advantages of droop type and inertia frequency controllers. A generalised linear small-signal prototype was also created to test the durability of the suggested PV power management loop. The proposed PV system model performed satisfactorily in the analysis, satisfying all active power control requirements of the grid standards.

Hossain et al. [24] presented a reliable control design solution for power-sharing in a distributed energy resource (DER) microgrid. The proposal incorporated doubly-fed induction generators powered by wind and photovoltaic (PV) panels. Each DER system for wind and solar is connected to a battery. The control strategy is divided into two parts: In addition to a multi-input & output controller that can control set reference reactive and active powers, there are two separate reactive and active power drooping controllers. It was observed that the energy controller functioned properly despite considerable disruptions and load changes during linked operations and islanding transients.

A unique virtual inertia control frequency control model for islanded microgrids was created by Hossam Ali et al. [14] and allows for frequency control loops while taking high renewable energy penetration into account (RESs). Contrary to earlier robust controllers like the CDM controller, the VI controller has a straightforward construction. The suggested CDM controller was compared to a reliable controller-based H-infinity approach and a newly constructed VI control-based CDM controller under various RESs and system parameter modifications. The results show that the robustness of the CDM controller, which uses VI control, outperforms the robustness of the H-infinity controller. The suggested controller was also better suited to handle major disruptions and high levels of system uncertainty.

The recurrent ANFIS method trains this nonlinear adaptive droop to handle uncertainty. This design uses the multi-objective Artificial Bee Colony (ABC) approach to pick membership function settings [15] intelligently. The simulation results showed that the adaptive fuzzy droop outperformed the PID and continuous droop when the microgrid was subjected to a load disturbance. Additionally, some collected data demonstrated that employing the learned optimum fuzzy droop via various real-world patterns significantly reduced settling time and enhanced the nadir point of frequency response under specific parameter uncertainties. Finally, this fuzzy droop demonstrated its ability to handle wind power fluctuation compared to conventional droop effectively.

According to the literature review, the practical instability of the system is a significant limitation of the MPPT controller of the frequency. There are some drawbacks to the controller-based grid system, including substantial output voltage ripple, poor anti-interference performance, and high THD content at the AC terminal. Load fluctuations, parameter uncertainty, high total harmonic distortion (THD), poor power factor, voltage fluctuations, poor power quality, voltage overshoot, slow dynamic response, lack of robustness, long response times, and difficult calculations are disadvantages of the approaches mentioned above. The Maximum Power Point Tracking (MPPT) and advanced Harris Hawk optimization (EHHO) methods for power and frequency control in low inertia systems are proposed to solve these problems.

3. Proposed Efficient Frequency Controller based on EHHO

The power system's available rotational inertia is decreased when converter-connected resources are used in place of conventional generation, leading to faster frequency dynamics and less stable frequency performance. A unit's proportionate electrical torque contribution to the ROCOF at its terminal is referred to as synthetic inertia. A grid characteristic, inertia, guards against frequency fluctuations when unexpected loads or generation changes happen. The suggested approach uses a variety of MPPT strategies to provide the most electricity because solar PV systems are pricey. Frequent controllers are chosen using the Entropy-based Harris Hawks Optimization (EHHO) Algorithm.

Convergence takes longer in this situation. Entropy calculations have a faster convergence and take less time than energy calculations. Synthetic inertia is activated when a significant amount of frequency shifts is found. It can be done by keeping an eye on the ROCOF, entering the absolute frequency value, and so forth, or looking for absolute deviations from the frequency moving average greater than a specific threshold. The proposed task requires a careful balancing act between activation delays, leaving the entrance into force, and unnecessary or unwanted limits. The schematic representation of the intended work is represented in Fig. 2.

The PV array is made up of several parallel strings. This port is where the converter is connected. In the converter design, a three-level IGBT bridge PWM controller is utilized. A tiny harmonics filter C and inverter choke RL filter the harmonics emitted by the IGBT (insulated-gate

bipolar transistor) Bridge. A 3-phase transformer links the utility distribution system to the inverter. An MPPT controller manages the inverter. The MPPT system automatically adjusts the inverter's VDC reference signal. The PV array model begins with an input luminescence of 1000 W/m^2 and an operating temperature of 45 °C. Supercapacitors are utilized in energy storage systems. Supercapacitors are ideal for a range of power applications requiring electrical output for short periods because of their large energy density. The supercapacitor has some active power reserve despite having no rotational kinetic energy. The supercapacitor can display a quick active power response while using the innovative active power control. So, to short-term inhibit the abrupt shift in frequency, the supercapacitor can be employed as an efficient energy storage device.

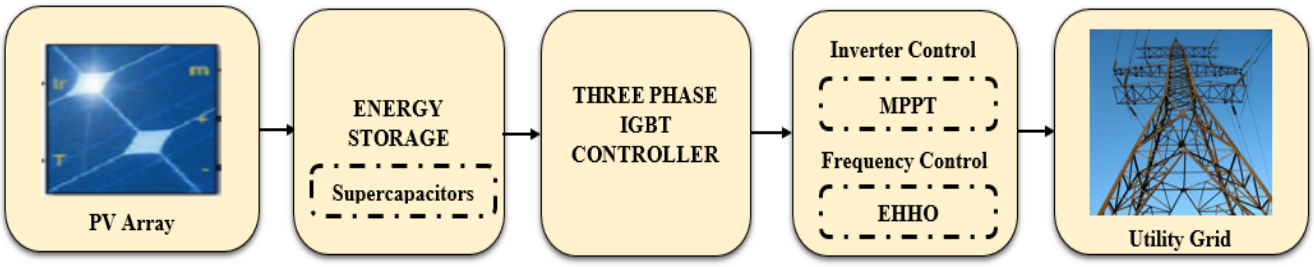

Fig. 2 Overall architecture of the proposed model

3.1. PV Array

A Solar photovoltaic plant integrating the voltage portion of the transmission system is depicted in Fig. 3.

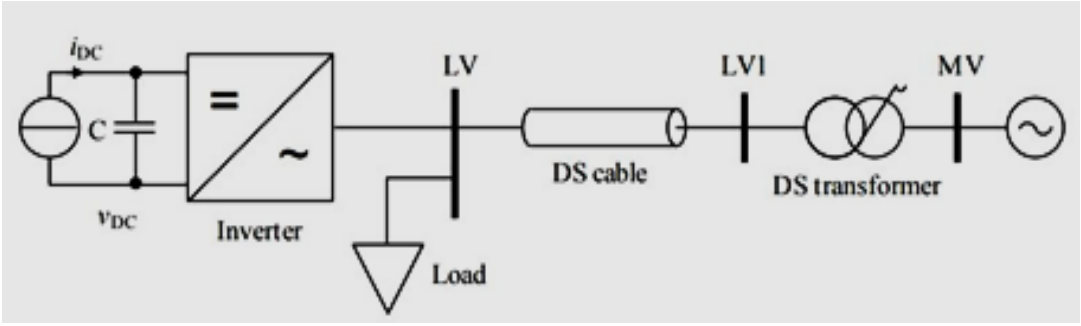

Fig. 3 PV generation single phase diagram

A feeder, a load, and a distribution transformer are also present. This unit consists of a three-phase energy source, PV array, two-level inverter and a control system. A capacitor C and a DC current source are needed to duplicate the PV array. The control system uses DC current and voltage management to regulate PV array characteristics and MPPT. The load and the PV power plant are connected in parallel. Without dynamic voltage control, steady-state voltage management is accomplished via transformer tap changers. Fig. 4 illustrates how the PV model [29] enhances computing performance.

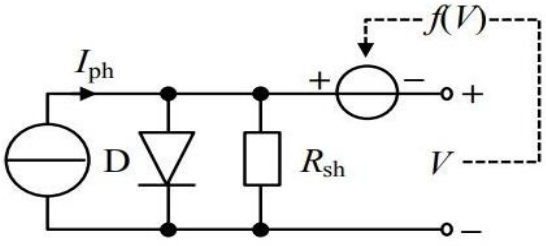

Fig. 4 Equivalent model for PV circuit

The associated Equation (1) and Equation (2) explain the behaviour of the I-V characteristic.

$$\boldsymbol{I = I_{ph} - I_s\left[e^{q\frac{f(V)}{N_s k_B T A}} - 1\right] - \frac{f(V)}{R_{sh}}} \quad (6)$$

$$\boldsymbol{f(V) = \alpha_0 + \alpha_1 V + \alpha_2 V^2 + \alpha_3 V^3} \quad (7)$$

Where q stands for the elementary charge (1.602176571019 C), kB for the Boltzmann constant (1.38064881023), T for the module's temperature, Ns for the number of series cells, I_{ph} for the photo-electric current, I_s for the saturation current, R_{sh} for the shunt resistance and A for the ideality factor. The parameters 0, 1, 2, and 3 for a specific module type can be determined. The characteristics of a PV array in terms of power and current with voltage are shown in Fig. 5a and 5b.

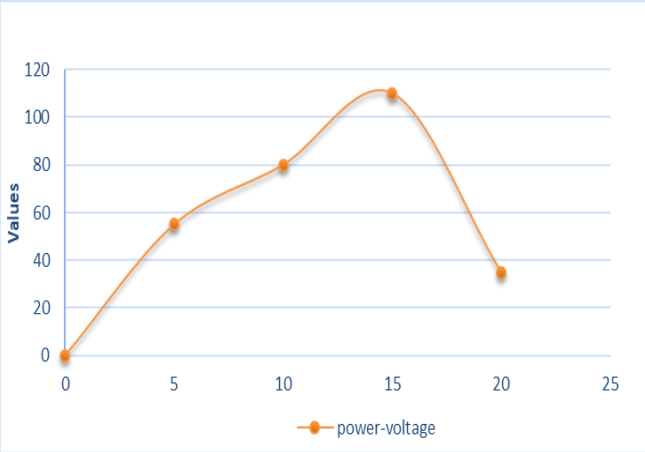

Fig. 5a Graphical plot for characteristics representation of power-voltage PV Array

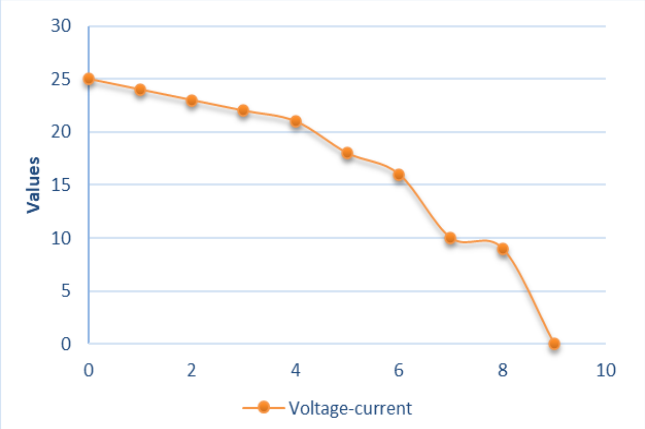

Fig. 5b Graphical plot for characteristics representation of current-voltage PV Array

3.2. 3-level IGBT bridge Controller

Single-phase grid-linked inverters come in two varieties: those with and without isolating transformers. The former offers better EMI performance than transformer-less inverters. Here, the first transformer is utilized. Fig. 6 shows a 3-phase grid connected inverter with six switches, a dc voltage source (V_{dc}), and a power grid (V_{grid}). For inverter-based DG, the output voltage of the inverter should be greater than V_{grid}. Power delivery to the grid is essential. Since V_{grid} is unregulated; controlling the current entering the system is the only way to control how it operates [17]. Fig. 7 shows a flow chart of the inverter controll23er algorithm.

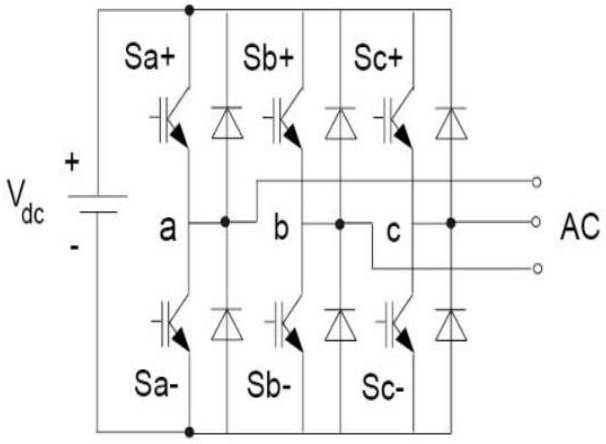

Fig. 6 Diagrammatic representation of 3-level PWM controller

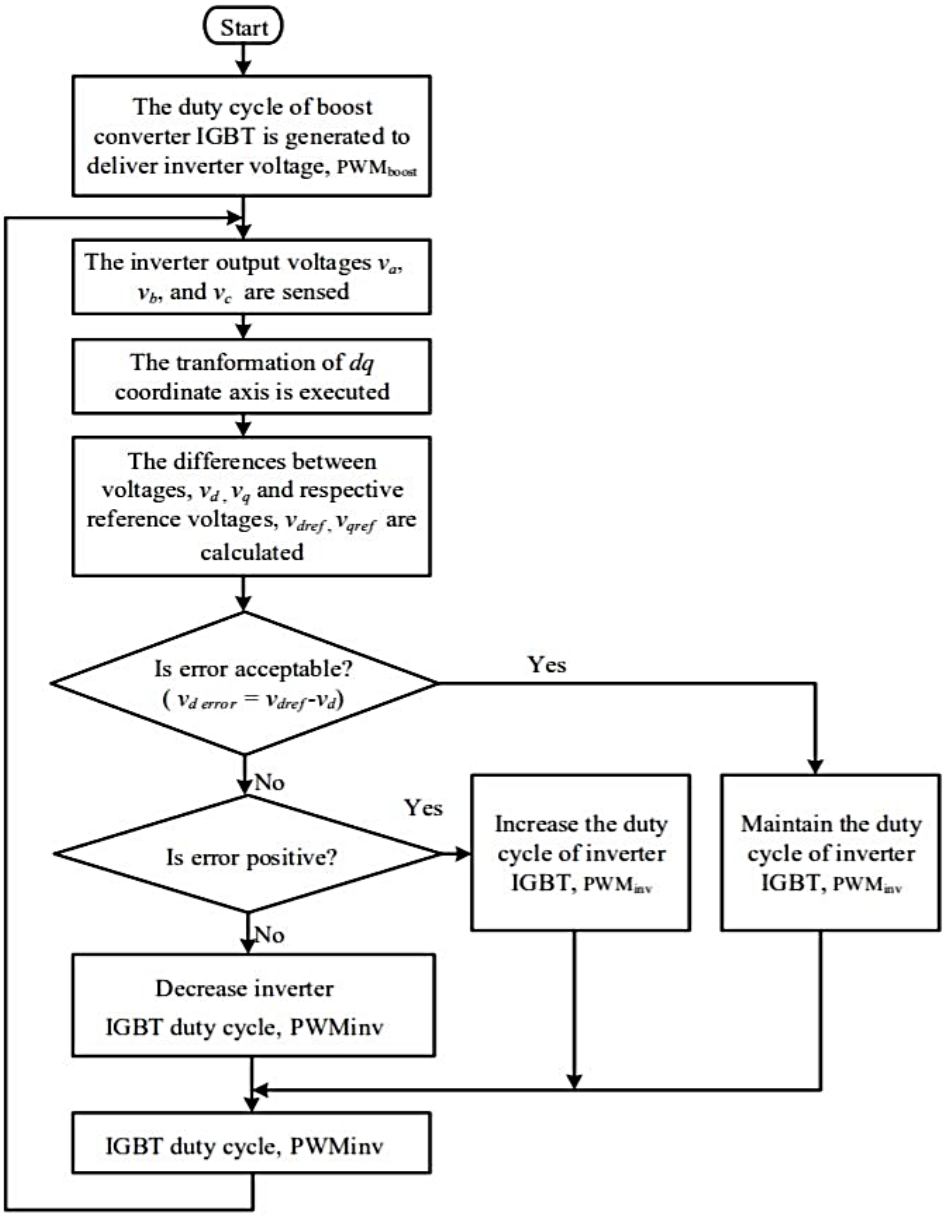

Fig. 7. Flowchart of the proposed controller algorithm

3.2.1. Power control via MPPT

To enable PV systems to function at their MPP in response to changes in their solar irradiation and temperature changes, an MPPT circuit must be linked between the PV module acting as an MPPT circuit and the load, as represented in Fig. 8. A DC-DC converter and a controller circuit make up an MPPT circuit. This study was conducted with a boost converter. The boost converter is controlled by the MPPT controller, which modifies the settings to ensure that, regardless of the load or environment, the maximum power from the PV source is provided [18].

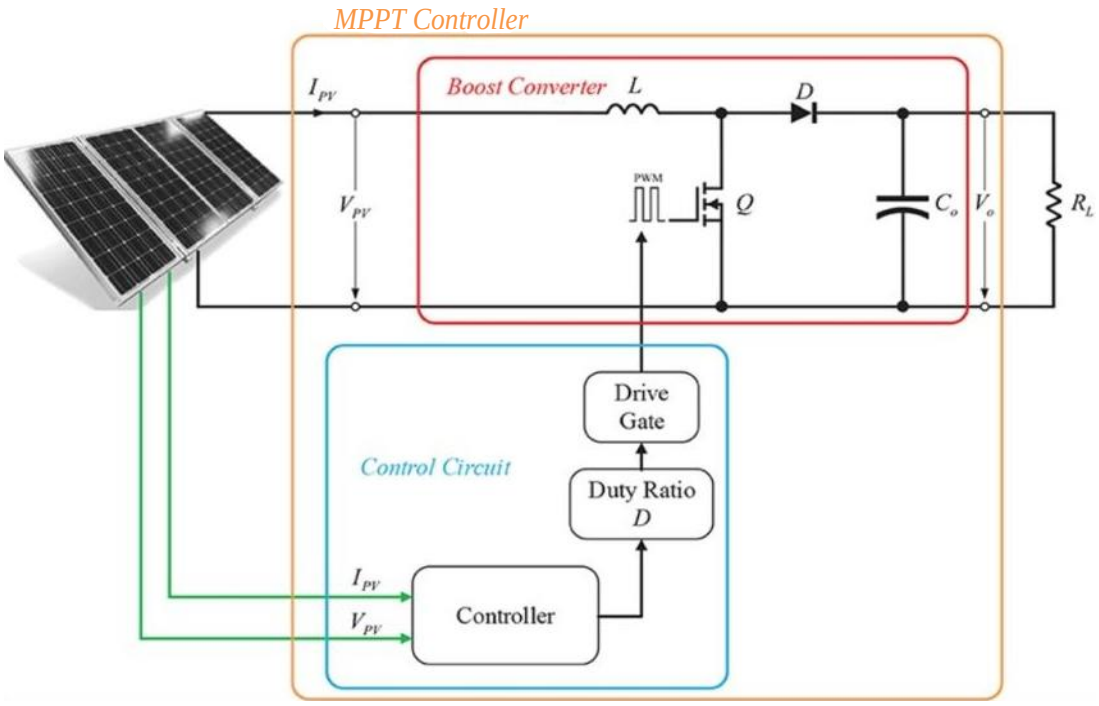

Fig. 8. MPPT-based solar PV system

To transform input voltage into a greater output value, the boost converter employs a switch (Q), an inductor (L), an output diode (D), and an output capacitor (Co). It clarifies why DC-DC converters function so effectively [19]. The MOSFET is referred to as the "Q" because it can be easily controlled using the PWM signal provided by the controller. The Q is switched on and off for each switching cycle, powering the boost converter. The inductor L stores energy when the switch "Q" is engaged during Ts' on-time Ton = DTs. The inductor "L" polarity is preserved when "Q" is switched off. A voltage difference between the input and output voltage results from the diode D sending the energy stored in the inductor L to the output capacitor "Co." Since the suggested converter has a significant gain; the working principle is only explored. The detailed study is provided below.

The equation mathematically represents the Boost converter's input and input voltage. It is because the boost converter runs in CCM mode (8).

$$V_o = \frac{1}{1-D} V_{PV} \tag{8}$$

where V_{PV} and V_0 are the MPPT boost converter's input and output voltages, respectively, and D is the PWM signal's duty cycle. The PV source's output current is the following:

$$I_{PV} = \frac{V_{PV}}{R_{eq}} = \frac{(1-D)V_o}{R_{eq}}. \tag{9}$$

Req is the name given to the comparable resistance located at the MPPT boost converter's input terminal. If the boost converter equipment functions properly, the conversion efficiency is 1.

$$\frac{V_{PV}^2}{R_{eq}} = \frac{V_o^2}{R_L}. \tag{10}$$

When Equation (5) is substituted for Equation (6), Req becomes:

$$R_{eq} = (1-D)^2 R_L. \tag{11}$$

The maximum power transfer theorem must be satisfied to provide maximum power point tracking. Fig. 9 shows a flow chart of the MPPT algorithm.

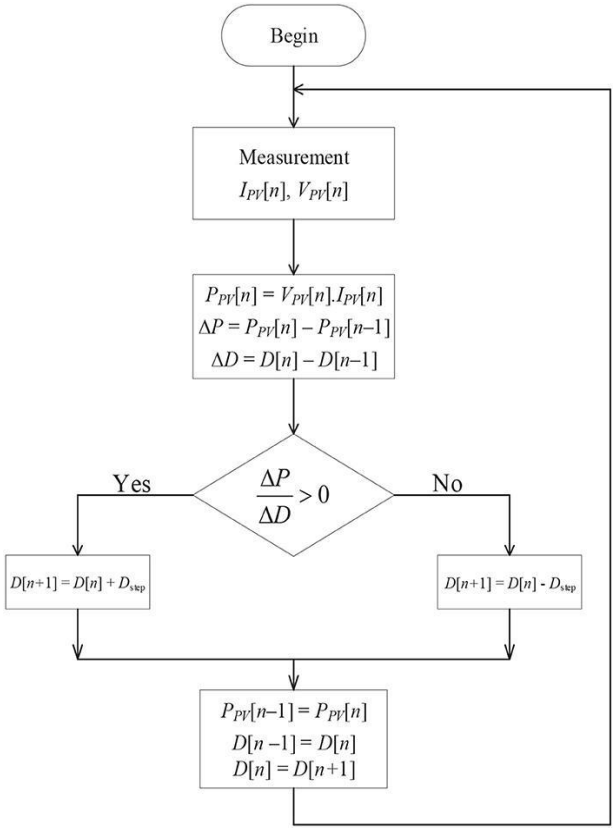

Fig. 9 Flowchart of MPPT algorithm

3.3. Frequency selection via EHHO

HHO is an optimization technique developed on Harris Hawk *behavioral* modelling. The key idea of the algorithm is that hawks cooperate to catch their prey. According to this algorithm, a swarm of Harris hawks strikes the target to surprise it from several perspectives. The Harris hawk's chase model is proportionate to the prey's escape strategy. When birds desire to attack, they work together.

The Harris hawks' leader engages in combat with the prey, follows it, and then disappears, leaving the subsequent Harris hawk to carry on the hunt. The target is exhausted by this technique, which leads to capture. The HHO approach performs better when applied to limited tasks than other algorithms. HHO can preserve the equilibrium between exploitation and exploration stages since it is a global optimizer. There are three steps in the HHO algorithm. The first step is the capacity for inquiry, which can be summed up as follows:

$$x(t+1) = \begin{cases} x_{\text{rand}}(t) - r_1 \mid x_{\text{rand}}(t) - 2r_2 x(tt \mid & q \geq 0. \\ x_{\text{prey}}(t) - x_a(t) - r_3(LB + r_4(UB - LB)) & q \prec 0. \end{cases} \quad (12)$$

where Hawk's current location is indicated by the letter X(t), and his future location is indicated by the letter X(t+1). Between t and $x_{\text{prey}}(t)(0,1)$ the iterations t, $x_{\text{prey}}(t)$, r_1, r_2, r_3, r_4, and q are random values (0,1). The Hawk that was randomly selected from the population is identified as $x_{\text{rand}}(t)$. Lower and upper bands are usually referred to by their respective abbreviations, LB and UB. The following is Harris Hawk's typical location, which is Xa(t):

$$x_2(t) = \frac{1}{N}\sum_{i=1}^{N} x_i(t) \quad (13)$$

Each Harris has a symbol of the form Xi(t). The position of the Harris Hawks has t iterations, and N' provides the total number of Harris Hawks. The period of exploitation then comes. The hawks lose energy as the chase and hunt go.

$$E = 2E_0\left(1 - \frac{1}{T}\right) \quad (14)$$

To figure out how much energy a prey has, apply the following formula:

The maximum number of repeats is T, E0 is the beginning energy, and E is the escaping energy. When this phase's ||E0|| ≥ 1 exploration and ||E0|| ≺ 1 exploitation activities occur. The third step is the exploitation phase, which focuses on improving local solutions based on those that have already been identified. This phase shows the Hawk's surprise attack on the prey from the previous phase. Four attack models have been created depending on the prey's flight and the hawks' pursuit. E0 stands for the beginning energy, T for the maximum number of repetitions, and E for the fleeing energy. When this phase's ||E0||≥ 1 exploration and ||E0||≺ 1 exploitation activities occur. Fig. 10 shows the HHO process in all of its several phases.

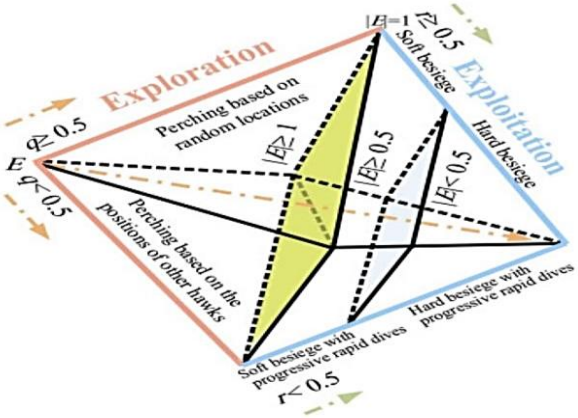

Fig. 10 The overall form of EHHO

4. Result and Discussion

The suggested system is developed utilizing the following machine configuration in the working platforms of MATLAB SIMULINK (version 20) and MATLAB PV LIB: The MATLAB SIMULINK working environment was used to replicate the Intel Core i3, OS: Windows 7, RAM: 4GB, and software characteristics. The fourth generation of computer languages gave rise to MATLAB (matrix laboratory), a multi-paradigm numerical calculation environment. The goal was to make scientific calculations and data input and output as simple as possible. The features supported by MATLAB include matrix multiplications, function and data visualization, algorithm implementation, user interface design, and compatibility with other languages, including C, C++, Java, and Python [21,22].
During two 8-second intervals, the sun's irradiation gradually increases from 200W/m2 to 1,000W/m2, keeping a steady temperature of 25°C or 45°C. Fig. 11 depicts the gradual variation in sun irradiation.

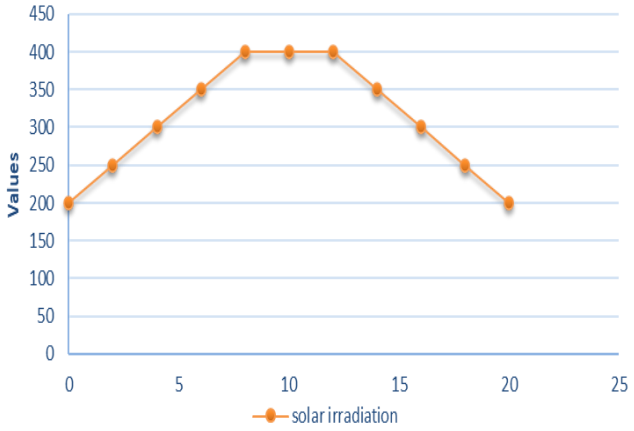

Fig. 11 Graphical representation of signal waveform vs of solar irradiation

The simulation results for PV system output power are proportional to solar irradiation and are roughly equal to PV panel output characteristics, as illustrated in Fig. 12a and 12b. When the MPP can be monitored in both directions under identical conditions of constant temperature (at 25°C and 50°C), and stable or quickly declining solar irradiance, MPPT systems using two distinct algorithms function equally well. In the case of a PV system with a sudden rise in solar irradiation, the suggested MPPT tracker may react and track the MPP satisfactorily; however, the P&O algorithm has limited dynamic tracking capabilities until the solar irradiation shift stabilizes.

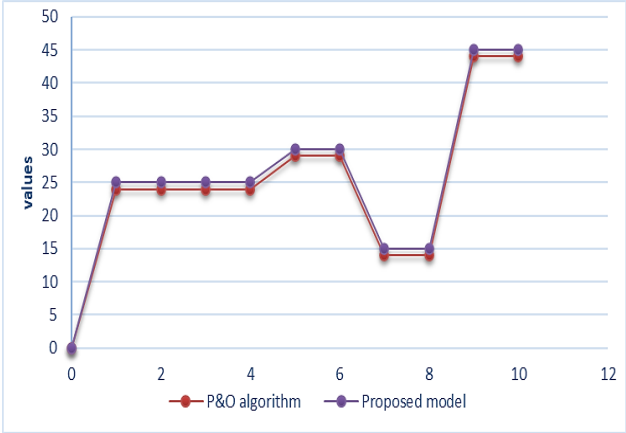

Fig. 12a. Graphical Comparison of the proposed model and P&O algorithm under 25°C

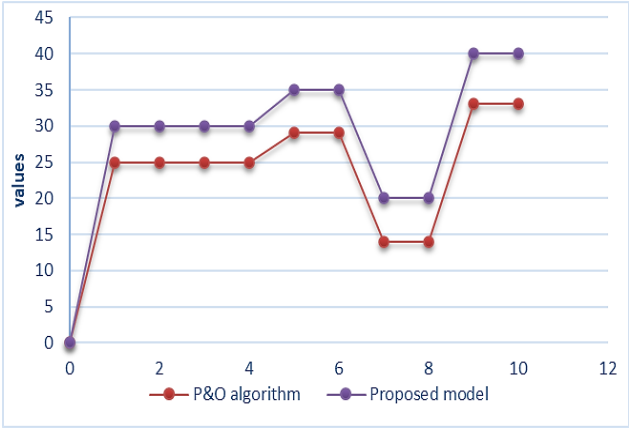

Fig. 12b. Graphical comparison of P&O model with the proposed under 45°C

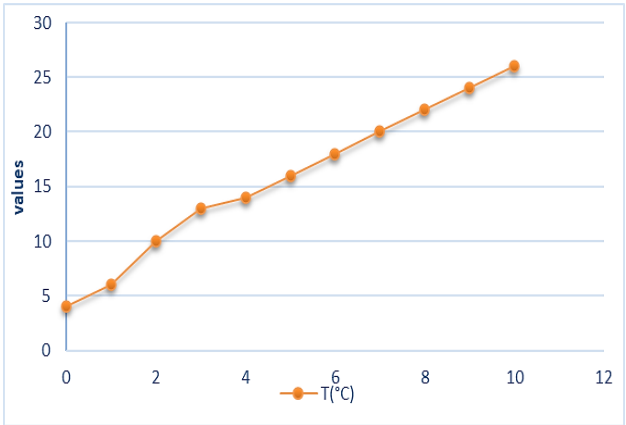

Fig. 13a. Graphical results for solar irradiation vs temperature change when it reduces to 25°C

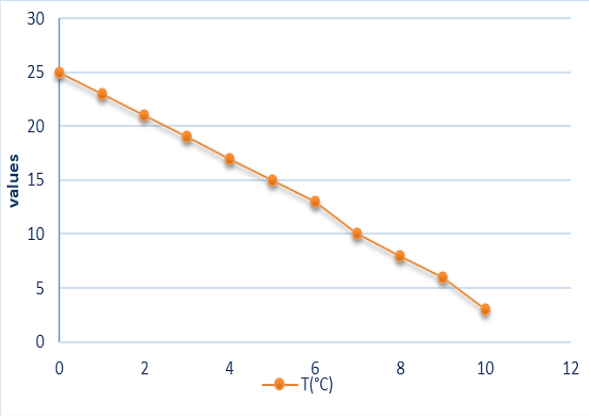

Fig. 13b Graphical results for change of solar irradiation vs temperature change when it settles down to 45°C

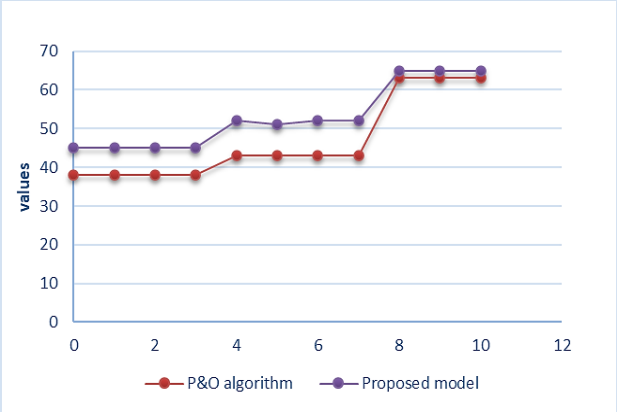

Fig. 14b Graphical representation of PV output power vs solar irradiation when increasing from 200W/m2 to 1000W/m2.

The quick shift in sun irradiation in this scenario. In actuality, the temperature of a PV cell fluctuates quite slowly. As a result, moderate temperature fluctuations are introduced in two separate situations. As demonstrated in simulation Fig. 13a and 13b, the temperature rises steadily over 9.5 seconds under the first condition, from 25℃ at t = 1 s to 45℃ at t = 10.5 s.

As demonstrated in Fig. 14a and 14b, a rapid increase in solar irradiation would provide a substantially larger rate of output power fluctuation to time duration during which power fluctuates (P/t) than the recommended technique would. The HHO algorithm, which is used in an integrated MPPT technique, also has this advantage.

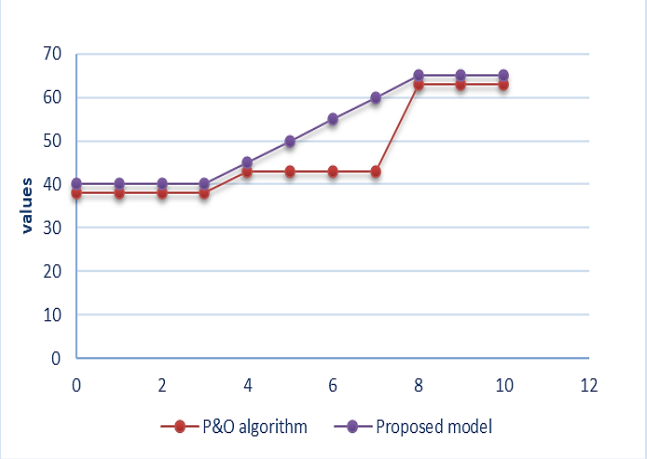

Fig. 14a. Graphical PV output in terms of power responses from 400W/m2 to 600W/m2

5. Conclusion

To increase frequency stability in low-inertia systems, this study used synthetic inertia. Because solar PV systems are expensive, the suggested approach utilizes various MPPT techniques to generate the most electricity possible. Frequency controllers are selected using the Harris Hawks Optimization Algorithm, which is entropy-based. Virtual inertia's efficacy in renewable energy sources and how much it enhances frequency stability are obvious in this research. Thus, this article provides an efficient model for solar PV arrays by fusing the MPPT and HHO algorithms. The experiment results were conducted in MATLAB and Simulink, showing a better aspect of the proposed model than the existing method, like the P&O algorithm. This paper will also be useful for other researchers to bring even integrated and advanced models that must focus on improving the grid-tier RES frequency stability.

Acknowledgements

The Author, with deep gratitude, would thank the supervisor for his guidance and constant support during this research.

References

[1] T. Kerdphol, F.S. Rahman, and Y. Mitani, "Virtual Inertia Control Application to Enhance Frequency Stability of Interconnected Power Systems with High Renewable Energy Penetration," *Energies*., vol.11, pp. 981, 2018.

[2] V. Pagola, R. Peña, J. Segundo, A. Ospino, "Rapid Prototyping of a Hybrid Pv-Wind Generation System Implemented in a Real-Time Digital Simulation Platform and Arduino," *Electroncis.*, vol.8, pp.102, 2019.

[3] D. Chen, Y. Xu, A.Q. Huang, "Integration of Dc Microgrids as Virtual Synchronous Machines Into the Ac Grid*," IEEE Trans. Ind. Electron.*, vol.64, pp.7455–7466, 2017.

[4] T. Kerdphol, F. S. Rahman, M. Watanabe, and Y. Mitani, "Robust Virtual Inertia Control of a Low Inertia Microgrid Considering Frequency Measurement Effects," IEEE *Access*., vol.7, pp. 57550-57560, 2019.

[5] W. J. Farmer, and A.J. Rix, "Optimising Power System Frequency Stability Using Virtual Inertia From Inverter-Based Renewable Energy Generation," *Iet Renewable Power Generation*., vol.14, no.15, pp.2820-2829, 2020.

[6] K. Y. Yap, C. R. Sarimuthu, and J. M. Y. Lim, "Grid Integration of Solar Photovoltaic System Using Machine Learning-Based Virtual Inertia Synthetization in Synchronverter," *IEEE Access.*, vol.8, pp.49961-49976, 2020.

[7] J. Zhao, X. Lyu, Y. Fu, X. Hu, & F. Li, "Coordinated Microgrid Frequency Regulation Based on Dfig Variable Coefficient Using Virtual Inertia and Primary Frequency Control," *IEEE Transactions on Energy Conversion.*, vol.31, no.3, 833-845, 2016.

[8] J. Liu, Y. Miura, and T. Ise, "Comparison of Dynamic Characteristics Between Virtual Synchronous Generator and Droop Control in Inverter-Based Distributed Generators," *IEEE Transactions on Power Electronics*., vol.31, no.5, pp. 3600-3611. 2015.

[9] Ch Venkata Ramesh, and A Manjunatha. "The Adequate Exploitation of Grid-Connected Single-Phase Photovoltaic Systems Unceasingly," *International Journal of Engineering Trends and Technology*, vol.70, no.5, pp. 120-130, 2022. Crossref, Https://Doi.Org/10.14445/22315381/Ijett-V70i5p215

[10] D. Chen, Y, Xu, and A. Q, "Huang, Integration of Dc Microgrids as Virtual Synchronous Machines Into the Ac Grid," IEEE *Transactions on Industrial Electronics.*, vol.64, no.9, pp. 7455-7466, 2017.

[11] H. Bevrani, B. François, and T. Ise, "Microgrid Dynamics and Control," *John Wiley & Sons*., 2017.

[12] Vijayalakshmi R, Pratheeba C, Sathyasree K, Ravichandran V , "Challenges, Issues and Solution for Hybrid Solar Pv and Wind Power Generation with Off-Grid Integration," *International Journal of Engineering Trends and Technology* , vol.68, no.3, pp.18-21, 2020, Https://Doi.Org/10.14445/22315381/IJETT-V68I3P204S.

[13] Vijaya Bhaskar K, Ramesh S, Chandrasekar P, "Evolutionary Based Optimal Power Flow Solution for Load Congestion Using Prng," *International Journal of Engineering Trends and Technology*, vol.69, no.8, pp.225-236, 2021, Https://Doi.Org/ 10.14445/22315381/IJETT-V69I8P228.

[14] Hossam Ali, Gaber Magdy, Binbin Li, G. Shabib, Adel A. Elbaset, Dianguo Xu and Yasunorimitani, "A New Frequency Control Strategy in An Islanded Microgrid Using Virtual Inertia Control-Based Coefficient Diagram Method", *IEEE Access*, vol.7, pp. 16979-16990, 2019.

[15] Ahmadreza Abazari, Masoudbabaei, S.M. Muyeenand Innocent Kamwa, "Learning Adaptive Fuzzy Drop of Pv Contribution of Frequency Excursion of Hybrid Micro-Grid During Parameters Uncertainties," *International Journal of Electrical Power & Energy Systems*., vol.123, pp.1-12, 2020,

[16] Ravindra Panchariya, Dr. Poonam Syal "An Improved Current Control Charging Scheme Using Neuro-Fuzzy and Fopid Based Mppt System for Ev Charging," *International Journal of Engineering Trends and Technology* , vol.69, no.10, pp.251-257, 2021.

[17] Malar, A. J. G., Kumar, C. A., & Saravanan, A. G, " Iot-Based Sustainable Wind Green Energy for Smart Cities Using Fuzzy Logic Based Fractional Order Darwinian Particle Swarm Optimization," *Measurement*, vol.166, pp.108208, 2020.

[18] X. Huang, D. Chang, C. Ling, and T. Q. Zheng, "Research on Single-Phase Pwm Converter with Reverse Conducting Igbt Based on Loss Threshold Desaturation Control," *Energies*, vol.10, no.11, pp.1845, 2017.

[19] Rai, B. Awasthi, S. Singh, and C. Dwivedi, "A Review of Maximum Power Point Tracking Techniques for Photovoltaic System," *Int. J. Eng. Res*., vol.5, pp. 539–545, 2016.

[20] Ahmad Hamdan Ariffin, Zeittey Karmilla Kaman, "Review on Consumers' Privacy and Economic Value Acceptance in Smart Grid Implementation," *International Journal of Engineering Trends and Technology*, pp.16-20, 2020.

[21] Malar, J. G., & Kumar, C. A, "Implementation of Mppt Techniques for Wind Energy Conversion System," *Internal Journal of Research and Analytical Reviews*, vol.5, no.3, 2018.

[22] H. Allouache1, A. Zegaoui, M. Boutoubat, A. A. Bokhtache1, F. Z. Kessaissia1, J.P. Charles, Et Al, "Distributed Photovoltaic Architecture Powering A Dc Bus: Impact of Duty Cycle and Load Variations on the Efficiency of the Generator," *in Aip Conference (Beirut)*, 2018.

[23] Appathurai, A., Carol, J. J., Raja, C., Kumar, S. N., Daniel, A. V., Malar, A. J. G., ... & Krishnamoorthy, S, " A Study on Ecg Signal Characterization and Practical Implementation of Some Ecg Characterization Techniques," *Measurement*, vol.147, pp.106384, 2019.

[24] Hossain, M., "Energy Management of Community Microgrids Using Particle Swarm Optimisation (Doctoral Dissertation, Unsw Sydney)," 2020.

[25] Sivasankari, B., and Ahilan, A. Smart Energy Harvesting for Intelligent Railway Condition Monitoring System," *Journal of Electrical Engineering*, vol.19, no.2, pp. 7-7, 2019.

[26] Sotirios I. Nanou, G. Apostolos, Papakonstantinou, and Stavros A. Papathanassiou, "A Generic Model of Two-Stage Grid-Connected Pv Systems with Primary Frequency Response and Inertia Emulation," *Electric Power Systems Research*., vol.127, pp. 186-196, 2015.

[27] M.A. Hannan, M.S.H. Lipu, P.J. Ker, R.A. Begum, V.G. Agelidis, and F. Blaabjerg, "Power Electronics Contribution to Renewable Energy Conversion Addressing Emission Reduction: Applications, Issues, and Recommendations," *Appl. Energy*, vol.251, pp.113404, 2019.

[28] Kah Yung Yap, R. Charles Sarimuthu and Joanne Mun-Yee Lim, "Grid Integration of Solar Photovoltaic System Using Machine Learning-Based Virtual Inertia Synthetization in Synchronverter", *IEEE Access.*, vol.8, pp. 49961-49976, 2020.

[29] Sivasankari, B., Ahilan, A., Jothin, R., & Malar, A. J. G, "Reliable N Sleep Shuffled Phase Damping Design for Ground Bouncing Noise Mitigation," *Microelectronics Reliability*, vol.88, pp.1316-1321, 2018.